EFFECT SIZE PROPORTIONS AND DISTANCES BETWEEN THE NON-METALLIC INCLUSIONS ON BENDING FATIGUE STRENGTH OF STRUCTURAL STEEL

LIPIŃSKI Tomasz, WACH Anna

University of Warmia and Mazury in Olsztyn, Olsztyn, Poland, EU
tomasz.lipinski@uwm.edu.pl, anna.wach@uwm.edu.pl

Abstract

Steel is the most popular structural material. The properties and practical applications of all constructional materials, including steel, are determined mostly by their structure. Non-metallic inclusions are one of the factors that influence the fatigue strength of steel. The physical and chemical reactions that occur in the process of steel melting and solidification produce non-metallic compounds and phases, referred to as inclusions. The quantity of non-metallic inclusions is correlated with the content of dopants in the alloy, while their phase composition and structure, in particular shape, dimensions and dispersion, are determined by the course of metallurgical processes.

The experimental material consisted of semi-finished products of high-grade, medium-carbon structural steel. The production process involved two melting technologies: steel melting in a 140-ton basic arc furnace with desulfurization and argon refining variants and in a 100-ton oxygen converter and next subjected to vacuum circulation degassing. Billet samples were collected to analyse the content of non-metallic inclusions with the use of an optical microscope and a video inspection microscope. The application of various heat treatment parameters led to the formation of different microstructures responsible for steel hardness values. Examination was realized on calling out to rotatory curving machine about frequency 6000 periods on minute. The objective of this study was to determine the influence of size proportions and distances between the fine non-metallic inclusions (up to 2 μm in size) on bending fatigue strength of high plasticity constructional steel. The results revealed that fatigue strength is determined by the analysed parameters and tempering temperature.

Keywords: Steel, high-grade steel, impurities, non-metallic inclusions, fatigue strength, bending fatigue strength

1. INTRODUCTION

Fatigue degradation is a type of damage that occurs over time and causes significant losses. Fatigue occurs and develops gradually due to cyclic service load that causes stress. When critical values are exceeded, the material cracks and becomes fit for scrap [1-4]. Processes that cause the material to crack under periodically varying loads are stochastic events. The above mentioned results mainly including material heterogeneity were caused by imperfections of the production process and its effect on alloy properties. As demonstrated by phenomenological research, the expansion of cracks resulting from fatigue is determined by the number of cycles, stress intensity and material properties. The combined effect of internal micro-stresses resulting from the presence of non-metallic inclusions in steel and stress may be caused by external load plays an important role in the formation and development of fatigue cracks. Internal stress is a function of the morphological composition of microstructures of steel, impurities and its morphology [5-9], micro-segregation [10-13] and the existing defects [4, 5, 14-17]. Distribution of non-metallic inclusions in steel and their quality is determined by various factors, including charge quality, process regime, furnace type and out-of-furnace processing [4-6]. The effect of sub-microscopic impurities on fatigue strength is much more difficult to analyse and is, therefore, less frequently investigated.

In a correctly performed metallurgical process, non-metallic inclusions in steel are randomly distributed, and their quantity can be described by the size proportions and distances between the impurities of structural steel α, which was investigated in the present study.

2.   AIM OF THE STUDY AND METHODS

The objective of this study was to determine changes in bending fatigue strength of steel hardened and tempered at different temperatures subject to the size proportions and distances between the impurities of structural steel.

The tested material comprised steel manufactured in three different metallurgical processes. The resulting heats differed in purity and size of impurities as non-metallic inclusions. Heat treatments were selected to produce heats with different microstructure of steel, from hard microstructure of tempered martensite, through sorbitol to the ductile spheroidized microstructure. In the first process, steel was melted in a 140-ton basic arc furnace. The study was performed on 21 heats produced in an industrial plant. The metal was tapped into a ladle, it was desulfurized and 7-ton ingots were uphill teemed. Billets with a square section of 100x100 mm were rolled with the use of conventional methods as a part of the second procedure. After tapping into a ladle, steel was additionally refined with argon. Gas was introduced through a porous brick, and the procedure was completed in 8-10 minutes. Steel was poured into moulds, and billets were rolled similarly as in the first method. In the third process, steel was melted in a 100-ton oxygen converter and deoxidized by vacuum. Steel was cast continuously and square 100x100 mm billets were rolled. Billet samples were collected to determine: chemical composition - the content of alloy constituents was estimated with the use of Leco analysers an AFL FICA 31000 quanto-meter and conventional analytical methods, relative volume of non-metallic inclusions with the use of the extraction method, dimensions of impurities by inspecting metallographic specimens with the use of a Quantimet 720 video inspection microscope under 400x magnification. It was determined for a larger boundary value of 2 μm. The number of particles in range of 2 μm and smaller was the difference between the number of all inclusions determined by chemical extraction and the number of inclusions measured by video method. Analytical calculations were performed on the assumption that the quotient of the number of particles on the surface divided by the area of that surface was equal to the quotient of the number of particles in volume divided by that volume [17].

It in aim of qualification of fatigue proprieties from every melting was taken 51 sections. The sections shapes of cylinder were about 10 mm in diameter. Their main axes be directed to direction of plastic processing simultaneously. It thermal processing was subjected was in aim of differentiation of building of structural sample. It depended on hardening from austenitizing by 30 minutes in temperature 880 °C after which it had followed quenching in water, for what was applied drawing. Tempering depended on warming by 120 minutes material in temperature 200, 300, 400, 500 or 600 °C and cooling down on air. Fatigue strength was determined for all heats. Heat treatment was applied to evaluate the effect of hardening on the fatigue properties of the analysed material, subject to the volume of fine non-metallic inclusions. The application of various heat treatment parameters led to the formation of different microstructures responsible for steel hardness values in the following range from 271 to 457 HV [4, 6]. Examination was realized on calling out to rotatory curving machine about frequency of pendulum cycles: 6000 periods on minute. For basis was accepted was on fatigue defining endurance level 10^7 cycles. The level of fatigue-inducing load was adapted to the strength properties of steel. Maximum load was set for steel tempered at a temperature of: 200 °C - 650 MPa, from 300 °C to 500 °C - 600 MPa, 600 °C - 540 MPa [4-6]. During the test, the applied load was gradually reduced in steps of 40 MPa (to support the determinations within the endurance limit). Load values were selected to produce 10^4-10^6 cycles characterizing endurance limits.

The arithmetic average size proportions and distances between the impurities of structural steel α were calculated with the use of the below formula (1):

$$\alpha = \frac{\bar{d}}{\lambda} \tag{1}$$

where: $\bar{d}$ - the average diameter of impurity, μm; λ - arithmetic average impurities space.

The each of the heats λ was calculated with the use of the below formula (2):

$$\lambda = \frac{2}{3} \bar{d} \left(\frac{1}{V_0} - 1 \right) \tag{2}$$

where: V_0 - the relative volume of sub-microscopic impurities, %.

The general form of the mathematical model is presented by equation (3)

$$z_{go} = a\alpha + b \tag{3}$$

where: z_{go} - bending fatigue strength; a, b - coefficients of the equation.

The significance of correlation coefficients r was determined on the basis of the critical value of the Student's t-distribution for a significance level α=0.05 and the number of degrees of freedom f = n-2 by formula (4).

$$t = \frac{r}{\sqrt{\frac{1-r^2}{n-2}}} \tag{4}$$

The values of the diffusion coefficient z_{go} near the regression line were calculated with the use of the below formula (5):

$$\delta = 2s\sqrt{1 - r^2} \tag{5}$$

where: s - standard deviation; r - correlation coefficient.

The values of the standard deviation s were calculated with the use of the below formula (6):

$$s = \sqrt{\frac{\sum(x - \bar{x})^2}{(n-1)}} \tag{6}$$

where: x- result of measurement; $\bar{x}$ - arithmetic average of measurement results.

3. RESULTS AND DISCUSSION

The chemical composition of analysed steel are presented in **Table 1**.

Table 1 Chemical composition of researched steel

| Process	Contents, wt %									
	C	Mn	Si	P	S	Cr	Ni	Cu	Mo	B
Arc furnace	0.25	1.03	0.18	0.022	0.019	0.54	0.45	0.19	0.25	0.002
Oxygen converter	0.24	1.13	0.27	0.018	0.018	0.56	0.5	0.02	0.26	0.003
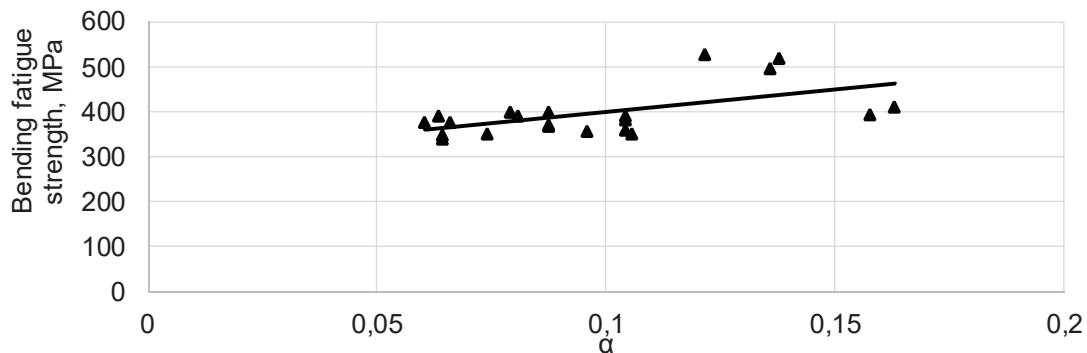
Fig. 1 Bending fatigue strength of steel hardened and tempered at 200 °C subject to size proportions and distances between the impurities

Bending fatigue strength of steel hardened and tempered at 200 °C in depends of size proportions and distances between the impurities are presented in **Fig. 1**, regression equation and correlation coefficients r in (7).

$$z_{go(200)} = 990.95\ \alpha + 301.69 \text{ and } r = 0.5666 \tag{7}$$

Bending fatigue strength of steel hardened and tempered at 300 °C in depends of size proportions and distances between the impurities are presented in **Fig. 2**, regression equation and correlation coefficients r in (8).
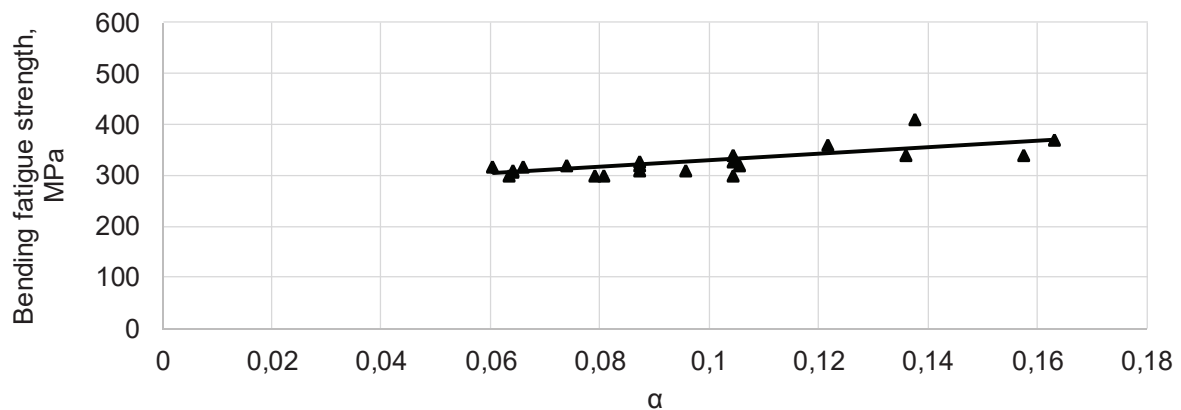
$$z_{go(300)} = 527.6\ \alpha + 292.99 \text{ and } r = 0.5385 \tag{8}$$
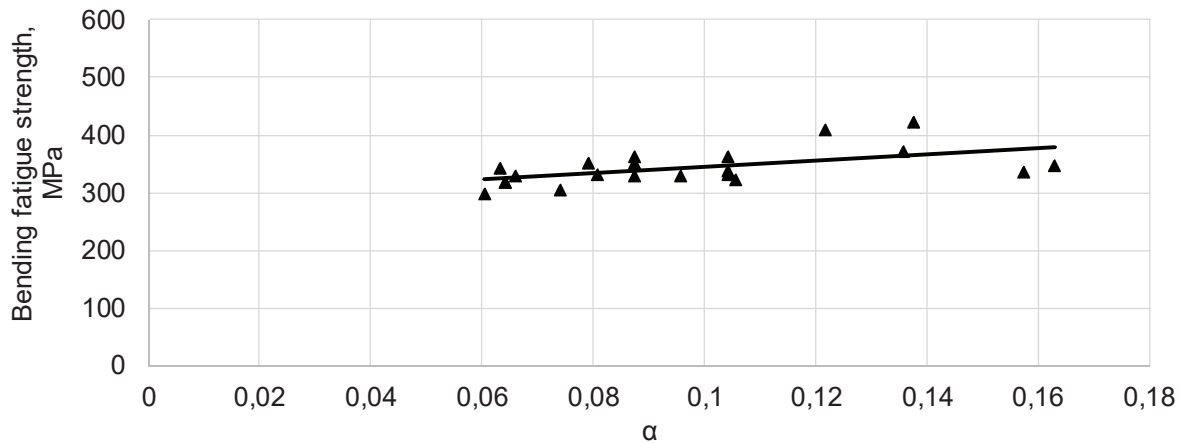
Fig. 2 Bending fatigue strength of steel hardened and tempered at 300 °C subject to size proportions and distances between the impurities

Bending fatigue strength of steel hardened and tempered at 400 °C in depends of size proportions and distances between the impurities are presented in **Fig. 3**, regression equation and correlation coefficients r in (9).

$$z_{go(400)} = 647.72\ \alpha + 265.97 \text{ and } r = 0.7326 \tag{9}$$

Fig. 3 Bending fatigue strength of steel hardened and tempered at 400°C subject to size proportions and distances between the impurities
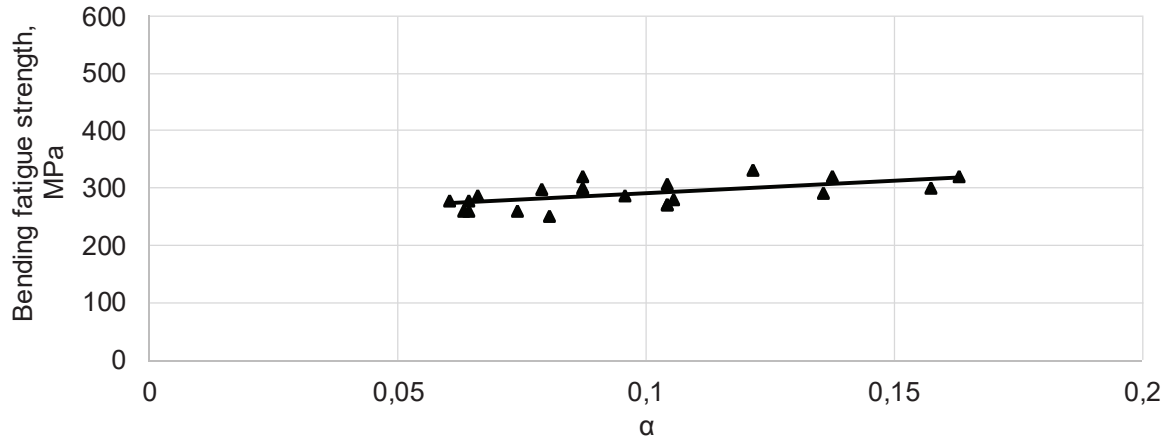
Bending fatigue strength of steel hardened and tempered at 500°C in depends of size proportions and distances between the impurities are presented in **Fig. 4**, regression equation and correlation coefficients r in (10).

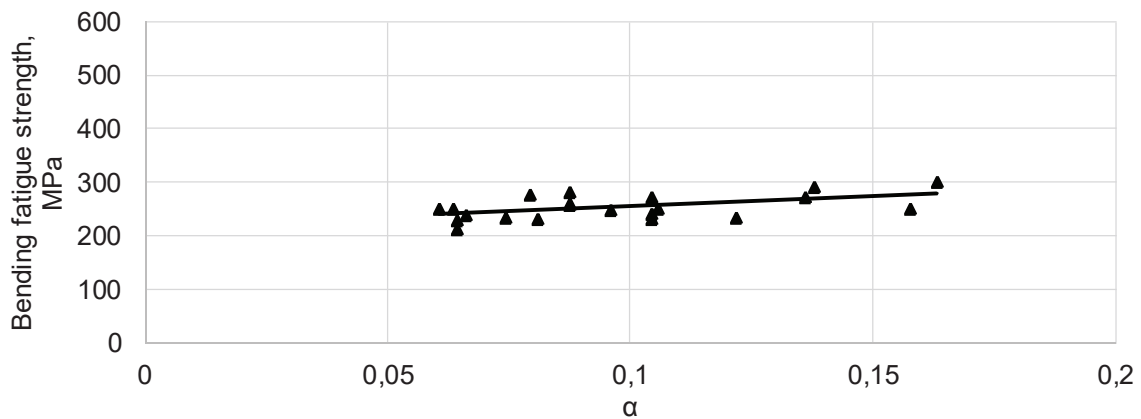$z_{go(500)}$ = 437.27 α + 249.01 and r = 0.5908 (10)

Bending fatigue strength of steel hardened and tempered at 600°C in depends of size proportions and distances between the impurities are presented in **Fig. 5**, regression equation and correlation coefficients r in (11).

$z_{go(600)}$ = 388.85 α + 217.24 and r = 0.5300 (11)

Parameters representing mathematical models and correlation coefficients are presented in **Table 2**.

Fig. 4 Bending fatigue strength of steel hardened and tempered at 500 °C subject to size proportions and distances between the impurities

Fig. 5 Bending fatigue strength of steel hardened and tempered at 600 °C subject to size proportions and distances between the impurities

Table 2 Parameters representing mathematical models and correlation coefficients

Tempering temperature °C	Regression coefficient a (3)	Regression coefficient b (3)	Correlation coefficient r	Degree of dissipation k around regression line δ (5)	$t_{\alpha=0.05}$ calculated by (4)	$t_{\alpha=0.05}$ from Student's distribution for p=(n-2)
200	990.95	301.69	0.5666	88.9912	2.997	
300	527.6	292.99	0.5385	50.5575	2.786	
400	647.72	265.97	0.7326	36.7556	4.692	2.093
500	437.27	249.01	0.5908	36.7909	3.192	
600	388.85	217.24	0.5300	38.6687	2.724	

4. CONCLUSIONS

The results of the study indicate that fatigue strength, represented by fatigue strength during rotary bending, is correlated with the size proportions and distances between the impurities measuring up to 2 µm. The presence of statistically significant correlations was verified by Student's t-test (5), **Table 2**.

With exception of 600 °C the higher the tempering temperature, the lower is the hardness of steel, and the smaller the dispersion of values around the regression line.

The results of the study indicate that the presence of non-metallic inclusions measuring up to 2 µm, represented by the quotient of *average diameter of impurity* and arithmetic average impurities space for sub-microscopic non-metallic inclusions α increases the magnitude of stress that induces fatigue cracking.

A positive correlation coefficient describing the relationships between bending fatigue strength and size proportions and distances between the impurities in **Figs. 2-10** (**Table 3**) indicates that the fatigue strength z_{go} increases with an increase in α (1).

The quotient of *average diameter of impurity* and arithmetic average impurities space for sub-microscopic non-metallic inclusions α was inversely proportional to the value of coefficient z_{go}. The above suggests that an increase in the diameter of impurity and/or decrease of impurities space λ of sub-microscopic inclusions in structural steel increases the value of z_{go}.

The use of the size proportions and distances between the impurities of structural steel α enhances the methodology for evaluating the influence degree of steel purity on fatigue strength of structural steel.

REFEENCES

[1] DHUA S.K., AMITAVA R., SEN S.K., PRASAD M.S., MISHRA K.B., JHA S. Influence of non-metallic inclusion characteristics on the mechanical properties of rail steel. JMEPEG 9, 2000, pp. 700-709.

[2] EJAZ N., RIZVI S.A. Cable failure resulted in the crash of a trainer aircraft. Engineering Failure Analysis, Vol. 17, 2010, pp. 394-402.

[3] NIENDORF T., DADDA J., CANADINC D., MAIER H.J., KARAMAN I. Monitoring the fatigue-induced damage evolution in ultrafine-grained interstitial-free steel utilizing digital image correlation, Materials Science and Engineering A, Vol. 517, 2009, pp. 225-234.

[4] LIPIŃSKI T., WACH A. The Effect of Fine Non-Metallic Inclusions on The Fatigue Strength of Structural Steel. Archives of Metallurgy and Materials, Vol. 60, No. 1, 2015, pp. 65-69.

[5] LIPIŃSKI T., WACH A. Influence of Outside Furnace Treatment on Purity Medium Carbon Steel. In METAL 2013: 23rd International Conference on Metallurgy and Materials. Ostrava: TANGER, 2014, pp. 738-743.

[6] LIPIŃSKI T., WACH A. Dimensional Structure of Non-Metallic Inclusions in High-Grade Medium Carbon Steel Melted in an Electric Furnace and Subjected to Desulfurization. Solid State Phenomena, Vol. 223, 2015, pp. 46-53.

[7] RASHID A.Z., PURBOLAKSONO J., AHMAD A., AHMAD S.A. Thermal fatigue analysis on cracked plenum barrier plate of open-cycle gas turbine frame. Engineering Failure Analysis, Vol. 17, 2010, pp. 579-586.

[8] RAJE N, SLACK T, SADEGHI F. A discrete damage mechanics, model for high cycle fatigue in polycrystalline materials subject to rolling contact. International Journal of Fatigue, Vol. 31, 2009, pp. 346-60.

[9] XU J., ZHANG Z.L., ŘSTBY E., NYHUS B., SUN D.B. Constraint effect on the ductile crack growth resistance of circumferentially cracked pipes. Engineering Fracture Mechanics, Vol. 77, 2010, pp. 671-684.

[10] WOŁCZYŃSKI W., KLOCH J. Mass Conservation for Microsegregation and Solute Redistribution in Cellular/Dendritic Solidification with Back-Diffusion. Materials Science Forum, Vol. 329/330, 2000, pp. 345-354.

[11] WOŁCZYŃSKI W., BOBADILLA M., DYTKOWICZ A. Segregation Parameters for Cells or Columnar Dendrites of Alloys with δ/γ Transformation during Solidification. Archives of Metallurgy and Materials, Vol. 45, 2000, pp. 303-308.

[12] CORNELIUS T., BIRGER K., NILS-GUNNAR I. Fatigue anisotropy in cross-rolled, hardened medium carbon steel resulting from mns inclusions. Metallurgical and Materials Transactions, Vol. 37A, 2006, pp. 2995-3007.

[13] ULEWICZ R. Quality control system in production of the castings from spheroid cast iron. Hutnik, Vol. 42, No. 1, 2003, pp. 61-63.

[14] SELEJDAK J., ULEWICZ R., INGALDI M. The evaluation of the use of a device for producing metal elements applied in civil engineering. In METAL 2013: 23rd International Conference on Metallurgy and Materials. Ostrava: TANGER, 2014, pp. 1882-1888.

[15] MURAKAMI Y., ENDO M. Effects of defects, inclusions and in-homogeneities on fatigue strength. International Journal of Fatigue, Vol. 16, No. 3, 1994, pp. 163-82.

[16] WOŁCZYŃSKI W. Thermodynamic Prediction of The Diffusion Barrier Morphology in The Al/Ni - Nano-Foil Designed For The Self-Propagating Reaction. Archives of Metallurgy and Materials, Vol. 62, 2015 (in print).

[17] Ryś J. Stereology of materials. FOTOBIT DESIGN, Krakow (1995) (in Polish).